

$^{26}\text{Si}(p, \gamma)^{27}\text{P}$ direct proton capture by means of the asymptotic normalization coefficients method for mirror nuclei

G. D'Agata^{1,*}, A. I. Kilic¹, V. Burjan¹, J. Mrazek¹, V. Glagolev¹, V. Kroha¹, G. L. Guardo²,
M. La Cognata², L. Lamia^{2,3,4}, S. Palmerini^{5,6}, R. G. Pizzone², G. G. Rapisarda², S. Romano^{2,3,4}, M. L. Sergi^{2,3},
R. Spartà^{2,3}, C. Spitaleri², I. Siváček^{1,7} and A. Tumino^{2,8}

¹*Nuclear Physics Institute of the Czech Academy of Sciences, 250 68 Řež, Czech Republic*

²*INFN - Laboratori Nazionali del Sud, Via Santa Sofia 62, 95123, Catania, Italy*

³*Dipartimento di Fisica e Astronomia "E. Majorana", Università degli Studi di Catania, Via Santa Sofia 64, 95123, Catania, Italy*

⁴*Centro Siciliano di Fisica Nucleare e Struttura della Materia (CSFNMS), Catania 77843, Italy*

⁵*Dipartimento di Fisica e Geologia, Università degli Studi di Perugia, via A. Pascoli s/n, 06123, Perugia, Italy*

⁶*INFN-sezione di Perugia, via A. Pascoli s/n, 06123, Perugia, Italy*

⁷*Flerov Laboratory of Nuclear Reactions, Joint Institute for Nuclear Research, 141980 Dubna, Russia*

⁸*Facoltà di Ingegneria ed Architettura, Kore University, Viale delle Olimpiadi, 1, I-94100 Enna, Italy*



(Received 20 October 2020; revised 11 December 2020; accepted 12 January 2021; published 25 January 2021)

The $^{26}\text{Si}(p, \gamma)^{27}\text{P}$ reaction might be relevant in understanding the ^{26}Si depletion and ^{26}Al production in stars. The asymptotic normalization coefficients (ANC) for the $^{26}\text{Si}(p, \gamma)^{27}\text{P}$ reaction were extracted earlier from the reanalysis of $^{26}\text{Mg}(d, p)^{27}\text{Mg}$ and $^{26}\text{Mg}(t, d)^{27}\text{Mg}$ reactions, in which the deduced ANC's show significant discrepancies. In this work, a dedicated (d, p) measurement is presented: the ANC for the $^{27}\text{Mg} \rightarrow ^{26}\text{Mg} + n$ virtual decay is deduced from the $^{26}\text{Mg}(d, p)^{27}\text{Mg}$ reaction populating the ground and the first excited state of ^{27}Mg using the distorted wave Born approximation (DWBA). The charge symmetry properties for mirror nuclei have been used to calculate the ANC for the direct capture $^{26}\text{Si} + p \rightarrow ^{27}\text{P}$ populating the ground state of ^{27}P . By means of the same formalism, the Γ_p width for the first excited state has also been deduced. The reaction rate is also updated using recent values for the Γ_γ/Γ_p ratio measured by [Sun *et al.*, *Phys. Rev. C* **99**, 064312 (2019); Sun *et al.*, *Phys. Lett. B* **802**, 135213 (2020)].

DOI: 10.1103/PhysRevC.103.015806

I. INTRODUCTION

The presence of ^{26}Al along the galactic plane in the first spectral images in γ -ray wavelength of our galaxy [1], has caught the attention of many physicists. Its origin has been heavily debated in the last 40 years. ^{26}Al presence has been detected using the 1.809 MeV γ -ray emission line from the deexcitation of the first excited state of ^{26}Mg , populated by the β^+ decay of ^{26}Al ($T_{1/2} = 0.72$ Myrs). This emission has been found in a large longitudinal range, with a major hot spot near the center of our galaxy and several other local maxima along the galactic plane [2,3]. The distribution of ^{26}Al suggests the hypothesis of its production in massive stars (see Ref. [4] and references therein). Different possible scenarios for ^{26}Al have been proposed, such as core-collapse supernovae, Wolf-Rayet objects, and AGB stars [5]. Also novae [6] and x-ray bursts [7] have been appointed to be a possible source of ^{26}Al . All those possible sites of production can enrich the interstellar medium with elements coming from proton capture. The nucleosynthesis reaction chain that is supposed to contribute the most to the ^{26}Al production is represented by the $^{24}\text{Mg}(p, \gamma)^{25}\text{Al}(\beta^+)^{25}\text{Mg}(p, \gamma)^{26}\text{Al}$ [8]. This scheme is

complicated by the presence of the well-known, short-lived isomeric state $^{26}\text{Al}^m$ ($T_{1/2} = 6.34$ sec), that can be produced in the same stellar environment: the knowledge of the exact ratio between $^{26}\text{Al}^s$ and $^{26}\text{Al}^m$ would be therefore important to better understand the amount and distribution of ^{26}Al throughout the galactic plane [9].

^{26}Al production can be bypassed by the competing $^{25}\text{Al}(p, \gamma)^{26}\text{Si}(\beta^+)^{26}\text{Al}^m$ reaction chain, in which ^{25}Al captures a proton, ending up mostly in the isomeric state [10]. Furthermore, the ^{26}Si produced in this way can also capture a proton via the $^{26}\text{Si}(p, \gamma)^{27}\text{P}$ reaction, interfering with both the $^{26}\text{Al}^m$ and ^{26}Al productions.

The $^{26}\text{Si}(p, \gamma)^{27}\text{P}$ reaction has been already studied in the past [11–16]. In particular, using the asymptotic normalization coefficient (ANC) method on data coming from Meurders and Van Der Steld [17] for the reaction $^{26}\text{Mg}(d, p)^{27}\text{Mg}$, Guo *et al.* [18] were able to calculate the ANC's for the reaction $^{26}\text{Si}(p, \gamma)^{27}\text{P}$, using the well-established procedure for mirror nuclei [19–23]. The authors retrieved the ANC for the ground, the first, and the second excited states of the $^{26}\text{Mg} + n \rightarrow ^{27}\text{Mg}$ process, and deduced the ANC for the proton capture to the ground state of $^{26}\text{Si} + p \rightarrow ^{27}\text{P}$ process, and Γ_p width for the first and second resonant states.

These results were challenged by Timofeyuk *et al.* [24], in which the authors deduced the ANC, using the same mirror

*dagata@ujf.cas.cz

nuclei procedure, reanalyzing the data for the $^{26}\text{Mg}(t, d)^{27}\text{Mg}$ reaction [25]. The ANC values for the neutron capture populating the ground and first excited states of the $^{26}\text{Mg}(n, \gamma)^{27}\text{Mg}$ extracted in this way were lower than those of Guo *et al.* [18]. The astrophysical S factor at zero energy of the $^{26}\text{Si}(p, \gamma)^{27}\text{P}$ reaction to the ground state has been also deduced, resulting in a value 1.7 times smaller than Guo *et al.* [18]. Timofeyuk *et al.* [24] also estimated the possible mirror symmetry breaking between ^{27}Mg and ^{27}P . More recently, a ratio between the γ and proton channels has been experimentally evaluated in $\Gamma_\gamma/\Gamma_p = 1.35 \pm 0.39$ [26,27], and the Γ_p width has been extracted using the Γ_γ value from literature [28]. These values allowed for a new evaluation of the reaction rate.

Aim and structure of the paper

The aim of the following paper is to address the discrepancies in the ANC values with a dedicated (d, p) reaction measurement: the $^{26}\text{Mg}(d, p)^{27}\text{Mg}$ reaction has been used to study the $^{26}\text{Mg}(n, \gamma)^{27}\text{Mg}$ by means of the ANC method. The procedure for mirror nuclei has then been employed to gain information on the $^{26}\text{Si}(p, \gamma)^{27}\text{P}$ direct capture. The experiment has been performed using the 19.2 MeV deuteron beam available at the U-120M isochronous cyclotron operated by CANAM infrastructure project at the Nuclear Physics Institute of the Czech Academy of Science (Řež, Czech Republic).

After a presentation of the ANC method and its extension for mirror nuclei, both the experimental apparatus and procedures will be explained in detail. The extracted differential cross sections for the $^{26}\text{Mg} + d$ and $^{26}\text{Mg} + n$ processes will be used to extract the optical model potential (OMP) parameters using the FRESKO code [29] in the context of the distorted wave Born approximation (DWBA). Finally, the results will be discussed and compared with previous ones.

II. METHOD

The ANC method represents a useful tool to study direct capture reactions of interest for astrophysics: in the case of a reaction between charged particles, a precise measurement of the cross section at low energy is in fact usually hampered by the presence of the Coulomb barrier. The indirect methods can overcome this problem.

Several of them were developed in the last decades to measure the cross sections of astrophysical interest at the so-called Gamow energies [30]. Among the most used ones we refer to the Coulomb dissociation method [31] and to the Trojan horse method (THM) [32,33].

The ANC method allows one to obtain the cross section of a peripheral direct capture reaction $A(a, \gamma)B$ in terms of the radial overlap integral of the X and B nuclei of the $A(X, Y)B$ transfer reaction (Fig. 1), where the nuclei X and A can be considered as $X = Y + a$ and $B = A + a$ [34–36]. This method has been widely used in the last 20 years to investigate proton [37], neutron [38], and α [39] direct captures in stellar environment.

The cross section for the $A(X, Y)B$ process in the special case of one nucleon transfer, can be parametrized—in dis-

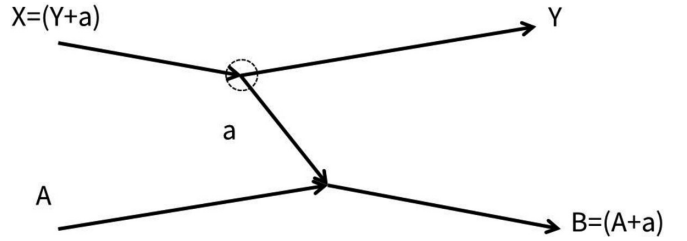


FIG. 1. Sketch of a general transfer reaction.

torted wave Born approximation (DWBA)—in terms of the product between the spectroscopic factors S for the initial and final states, when they are associated with a specific nucleon bound state [40]:

$$\frac{d\sigma}{d\Omega} = \sum_{j_B, j_X} S_{Aa, l_B, j_B} S_{Ya, l_X, j_X} \sigma_{l_B, j_B, l_X, j_X}^{\text{DWBA}}. \quad (1)$$

Taking into account the vertex $A + a \rightarrow B$ of the reaction in Fig. 1, the radial overlap function can be approximated by the wave function of the bound state ($B = A + a$) [41]:

$$I_{Aa, l_B, j_B}^B(r_{Aa}) = S_{Aa, l_B, j_B}^{1/2} \phi_{Aa, l_B, j_B}(r_{Aa}), \quad (2)$$

ϕ_{Aa, l_B, j_B} being the bound-state wave function of the relative motion between A and a , and $S_{Aa, l_B, j_B}^{1/2}$ the spectroscopic factor of the $(A + a)$ configuration with quantum numbers l_B and j_B inside the nucleus B . On the other hand, the radial overlap wave function in the asymptotic limit can be described as follows [41]:

$$I_{Aa, l_B, j_B}^B \xrightarrow{r_{Aa} > R_n} C_{Aa, l_B, j_B}^B \frac{W_{-\eta, l_{Aa}+1/2}(2k_{Aa}r_{Aa})}{r_{Aa}}, \quad (3)$$

while the asymptotic behavior of the bound-state wave function of the ($B = A + a$) final state can be expressed as

$$\phi_{Aa, l_B, j_B}^B \xrightarrow{r_{Aa} > R_n} b_{Aa, l_B, j_B}^B \frac{W_{-\eta, l_{Aa}+1/2}(2k_{Aa}r_{Aa})}{r_{Aa}}. \quad (4)$$

In both Eqs. (3) and (4), the $W_{-\eta, l_{Aa}+1/2}$ stands for the Whittaker function that describes the asymptotic behavior of the bound-state wave function for two charged interacting particles, η being the Sommerfeld parameter. The C_{Aa, l_B, j_B}^B coefficient of Eq. (3) is the ANC, while b in Eq. (4) is the so-called SPANC (single-particle ANC) and represents the normalization constant of the radial single-particle bound-state wave function tail. This quantity is therefore strongly tied to the single-particle potential used to reproduce the bound states of the nuclear system $B = A + a$ (usually a Woods-Saxon potential).

The same is valid for the other vertex of the sketch shown in Fig. 1, and using Eqs. (3) and (4) in Eq. (2), the cross section [Eq. (1)] can finally be modeled as follows:

$$\begin{aligned} \frac{d\sigma}{d\Omega} &= \sum_{j_B, j_X} (C_{Aa, l_B, j_B}^B)^2 (C_{Ya, l_X, j_X}^X)^2 \frac{\sigma_{l_B, j_B, l_X, j_X}^{\text{DWBA}}}{b_{Aa, l_B, j_B}^2 b_{Ya, l_X, j_X}^2} \\ &= \sum_{j_B, j_X} (C_{Aa, l_B, j_B}^B)^2 (C_{Ya, l_X, j_X}^X)^2 \times R_{l_B, j_B, l_X, j_X}, \end{aligned} \quad (5)$$

where the $\sigma_{l_B, j_B, l_X, j_X}^{\text{DWBA}}$ stands for the model cross section used to reproduce the angular distribution in DWBA.

In the case of proton (p) and neutron (n) transfer, the proton ANC (C_p^{A+p}) for the process $A + p \rightarrow B$ can be derived from a suitable mirror partner $D + n \rightarrow E$ —where D and E have inverted number of protons and neutrons with respect to A and B —using the relation [19–23]:

$$(C_p^{A+p})^2 = R_{\text{mirr}} (C_n^{D+n})^2. \quad (6)$$

The C_n^{D+n} coefficient is the neutron ANC of the mirror process and R_{mirr} is equal to

$$R_{\text{mirr}} = \left| \frac{F_l(ik_p R_N)}{k_p R_N j_l(ik_n R_N)} \right|^2, \quad (7)$$

$F_l(ik_p R_N)$ being the regular Coulomb function at imaginary momentum ik_p , $j_l(ik_n R_N)$ the spherical Bessel function of the l th order at imaginary momentum ik_n , and $R_N = 1.3 \times A^{1/3}$ fm (with A the atomic mass number of the A nucleus) the radius of the strong interaction between the proton and the A core. Varying the coefficient in R_N by 10%, the variation of R_{mirr} is less than 4%. The quantities k_p and k_n are related to the proton and neutron separation energies $-\varepsilon_p$ and ε_n , respectively, via the relation $k_{p(n)} = \sqrt{2\mu_{p(n)}\varepsilon_{p(n)}/\hbar}$, where μ_p and μ_n are the reduced mass of the $A + p$ or $D + n$ systems, respectively. The quantity R_{mirr} can be also calculated in a less general way using the spectroscopic factors S_p and S_n : the ANC values for both the proton and neutron channels can be written as $C_{p(n)} = \sqrt{S_{p(n)}} b_{p(n)}$, and assuming—for both the p and n mirror states—that both single-particle wave functions are the same in the nuclear interior, the quantity R_{mirr} can be extracted from the relation [42]

$$R_{\text{mirr}} = \left| \frac{b_{p(n)}}{b_{n(p)}} \right|^2. \quad (8)$$

In this way the ratio in Eq. (8) will also be weakly dependent on the chosen potentials. Using this theoretical framework, the $^{26}\text{Si}(p, \gamma)^{27}\text{P}$ reaction will be studied from the $^{26}\text{Mg}(n, \gamma)^{27}\text{Mg}$ mirror pair. The ^{27}Mg – ^{27}P mirror pair, however, has been suggested as a possible case of symmetry breaking [24], leading to different values of S_p and S_n . To verify this, a direct measurement on the $^{26}\text{Si}(p, \gamma)^{27}\text{P}$ would be needed.

III. EXPERIMENT

The experimental setup consisted of five $\Delta E - E$ telescopes, each of them consisting of a thin (250 μm) and a thick (5000 μm) silicon detector. Three of those telescopes, placed on one side of the beam axis (Fig. 2) and fixed to a rotating plate, had a $1 \times 3 \text{ mm}^2$ collimator in front of them and were placed at a distance of 183 mm from the target, with a 10° step between each other. Thanks to the rotating plate, those detectors covered the angular range between 7° to 60° at steps of 2° . By means of these telescopes it was possible to retrieve the angular distributions of the outgoing deuterons from the elastic scattering and the protons related to the ground and first

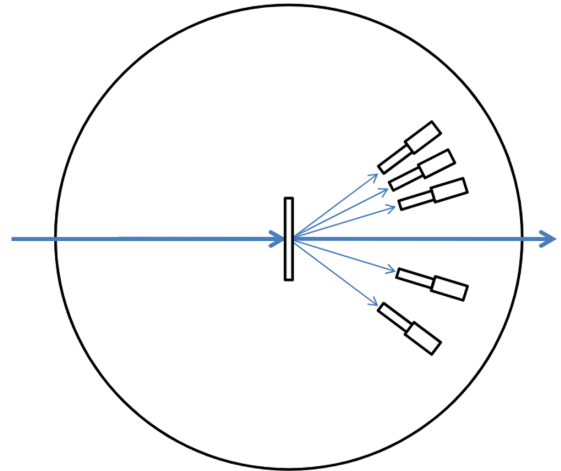


FIG. 2. Experimental setup.

excited state of ^{27}Mg . The other two detectors were mounted on a fixed plate and placed on the other side of the beam at 17° and 37° , respectively. These served as monitors to check the beam purity and alignment during calibration and data acquisition phases.

The deuteron beam ($E = 19.2 \text{ MeV}$, $I \approx 14 \text{ nA}$) impinged on a ^{26}MgO target ($70 \mu\text{g}/\text{cm}^2$) evaporated on a carbon backing ($32 \mu\text{g}/\text{cm}^2$) provided by the target laboratory of the Laboratori Nazionali del Sud - Istituto Nazionale di Fisica Nucleare (LNS–INFN). The energy resolution for the $\Delta E - E$ telescopes has been deduced from elastic scattering on pure ^{12}C and from standard α source, and has been found to be around 0.3%, while to estimate angular resolution the intrinsic precision of the rotating plate step and the kinematic straggling have been used ($\approx 0.25^\circ$ considering both the contributions).

The elastic scatterings of deuterons from other species (the oxygen contained in the target and the carbon backing) have small energy difference at low angles ($\leq 15^\circ$) with respect to the $^{26}\text{Mg} + d$ elastic scattering (0.02 MeV and 0.08 MeV at 12° , respectively). To separate the different contributions, several measurements have been conducted, delivering the same beam on solid targets made of ^{12}C and Mylar (to evaluate the elastic scattering on carbon), and a on a gas target filled with oxygen (isotopic purity $\approx 99\%$, pressure 150 mbar). Normalizing the yields of the elastic scattering of deuterons for the four different targets it was possible to subtract the contribution of C and O elastic scattering from the pure $^{26}\text{Mg} + d$ one. As it can be seen in Fig. 3, the measurement of the elastic scattering $^{16}\text{O} + d$ has a worse resolution than the other two. This occurs because of the gas cell used as oxygen target (5.2 cm radius). The angular and energy straggling of the outgoing deuterons had larger overall uncertainty, and the error over the scattering peak results to be circa 1.6 times higher. Nonetheless, the measurement still allowed us to estimate the oxygen contribution to the total elastic scattering cross section. Furthermore, the elastic scattering on oxygen coming from a Mylar target has also been used, in order match the information of the gas target thickness.

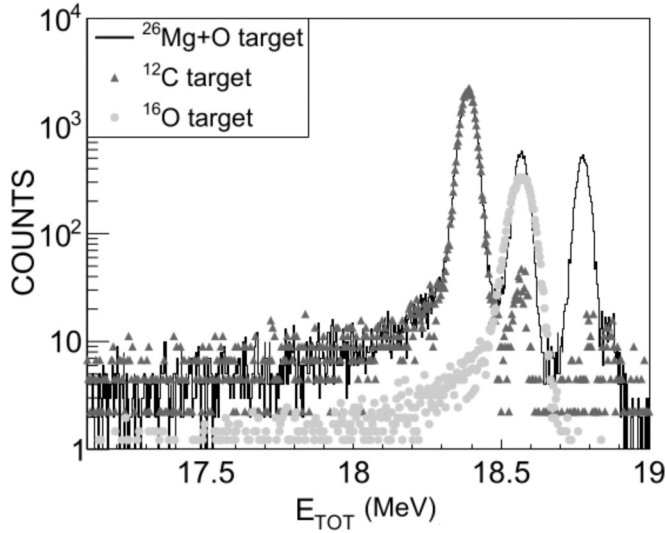


FIG. 3. Comparison between the contributions to elastic scattering from the $^{26}\text{Mg}+\text{O}$ (black line), pure ^{12}C (dark gray triangles), and ^{16}O gas target (gray circles) at 27° . The contribution from carbon and oxygen can be subtracted to obtain the pure magnesium one.

IV. DATA ANALYSIS AND ANC EXTRACTION

A. DWBA analysis

Among direct transfer reactions, many one-step particle transfer processes can be successfully described in terms of finite-range DWBA. The direct reaction mechanism can be used as a first approximation to describe the angular distributions and the total cross section. To retrieve the OMP of both the entrance and exit channels, the code FRESKO [29] has been used, and the results have been checked using DWUCK-5 [43]. The parameters for the entrance channel were extracted by fitting the elastic scattering angular distributions, while the exit ones have been deduced fitting the proton angular distributions for the ground and first excited states of ^{27}Mg . The selected optical model is

$$U = V_c(r_c) - V_0 f(x_0) - \left[W f(x_w) - 4W_D \frac{d}{dr} f(x_D) \right] + \frac{\hbar^2}{m_\pi c} V_{LS}(L\sigma) \frac{1}{r} \frac{d}{dr} f(x_{LS}). \quad (9)$$

In the equation above $V_c(r_c)$ is the Coulomb potential, V_0 and V_{LS} are the depth of the real volume and spin-orbit potentials, while W and W_D are the depth of volume and surface terms for the imaginary part of the potential, respectively. The function $f(x_i)$ represents the radial form of the Woods-Saxon potential, which can be written as $f(x_i) = (1 - e^{x_i})^{-1}$, x_i being equal to $(r - r_i A^{1/3})/a_i$, with r_i and a_i the radius and diffuseness parameters respectively, and A the atomic mass number. The function $f(x_i)$ is used as the radial part of the different potential terms, and the subscript i indicates each of the various contribution terms: 0 for the real volume, LS for the spin orbit, D for the surface and w for the volume term of the imaginary potential.

TABLE I. OMP parameters used in DWBA calculation. The D column refers to the entrance channel. The P1 and P2 columns refer to the two different potentials for the exit channel. As shown in Fig. 4 the two potentials describe both the ground and first excited states. As seed parameters for our calculations, we used P1 and P2 sets of potentials from Guo *et al.* [18].

Set	D	P1	P2
V_0 [MeV]	88.500	48.140	48.140
r_r [fm]	1.085	1.058	1.010
a_r [fm]	0.850	0.650	0.750
W_D [MeV]	13.250	7.850	27.850
r_D [fm]	1.300	1.250	1.350
a_D [fm]	0.650	0.650	0.500
V_{LS} [MeV]		6.200	6.200
r_{LS} [fm]		1.010	1.010
a_{LS} [fm]		0.750	0.750
r_c [fm]	1.300	1.300	1.300

The adopted OMP parameters are reported in Table I and the fitted curves obtained for the elastic channel $^{26}\text{Mg} + d$ and for the ground ($E_x = 0$ MeV, $J^\pi = \frac{1}{2}^+$) and first excited states ($E_x = 0.984$ MeV, $J^\pi = \frac{3}{2}^+$) are shown in Fig. 4, along with the experimental data. The spectroscopic factors were calculated using standard geometrical parameters $r_0 = 1.25$ fm and $a = 0.65$ fm. The transitions to the ground and first excited states are well described within the experimental errors, especially around the first maxima.

B. Results and discussions

The peripheral character of the $^{26}\text{Mg}(d, p)^{27}\text{Mg}$ reaction must be ascertained in order to apply the ANC method.

The peripheral property of the reaction used is documented by the weak dependence of the C^2 value from the geometry of the Woods-Saxon potential. If the reaction is peripheral, then the product $S_{\text{exp}} \cdot b^2 = C^2$ (where S_{exp} is the experimental spectroscopic factor) should have low sensibility while varying the b parameter, which would not be the case for S [44–48]. Using the OMP parameters P1 of Table I and varying the geometry of the Woods-Saxon well (r_0 and a), we found that while the spectroscopic factor varies by $\approx 55\%$, the C_{exp}^2 varies only $\approx 13\%$ (Fig. 5). The reaction can therefore be considered peripheral.

As it has been stated in Sec. II the expression for the $^{26}\text{Mg}(d, p)^{27}\text{Mg}$ reaction contains also the ANC for the virtual decay $d \rightarrow p + n$. Its value $C_{pn}^2 = 0.77$ fm $^{-1}$ was deduced from the Reid soft core potential [49], and used in other works [38,50,51].

The spectroscopic factors and ANC's retrieved from our experimental data are presented in Table II, where the errors are estimated taking into account the uncertainties of R [Eq. (5)] related to the statistical error of the experimental data and to the fitting procedure used to retrieve the OMP (15%): our ANC value is in agreement with Timofeyuk *et al.* [24], while not with Guo *et al.* [18].

To calculate the mirror ANC for the ground state of the $^{27}\text{P} \rightarrow ^{26}\text{Si} + p$, we applied Eqs. (6) and (7): the ANC for the

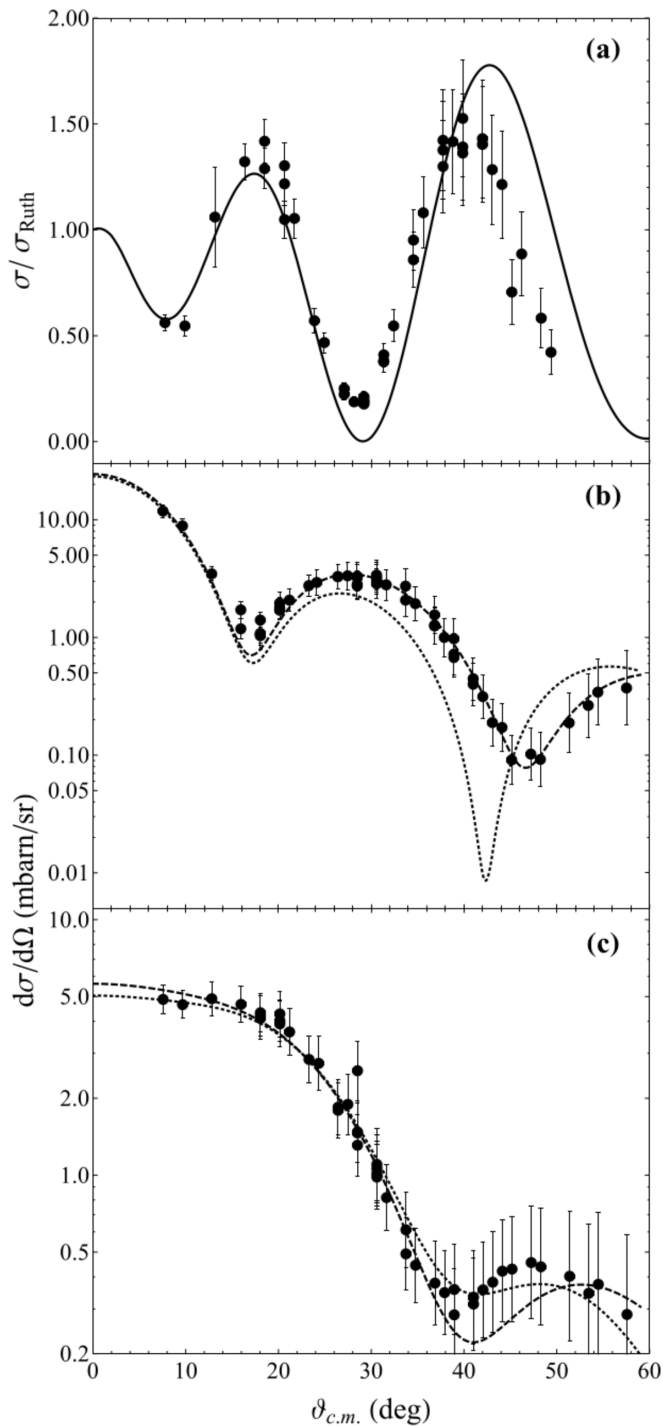


FIG. 4. Angular distributions for the (a) $^{26}\text{Mg} + d$ elastic scattering normalized to Rutherford scattering, for the (b) $^{26}\text{Mg}(d, p)^{27}\text{Mg}$ reaction ground state ($E_x = 0$ MeV, $J^\pi = \frac{1}{2}^+$), and for (c) first excited state ($E_x = 0.984$ MeV, $J^\pi = \frac{3}{2}^+$) and the DWBA calculations. All curves are compared with the current experimental data. The solid line is extracted using the potential D in Table I, while the dashed and dotted lines are calculated using P1 and P2, respectively.

capture in the ground state is then equal to $|C_{\text{exp}}^{1/2+}|^2 = 1420 \pm 255 \text{ fm}^{-1}$, value that is higher than the $1058 \pm 273 \text{ fm}^{-1}$ from Timofeyuk *et al.* [24] and lower than the $1840 \pm 240 \text{ fm}^{-1}$

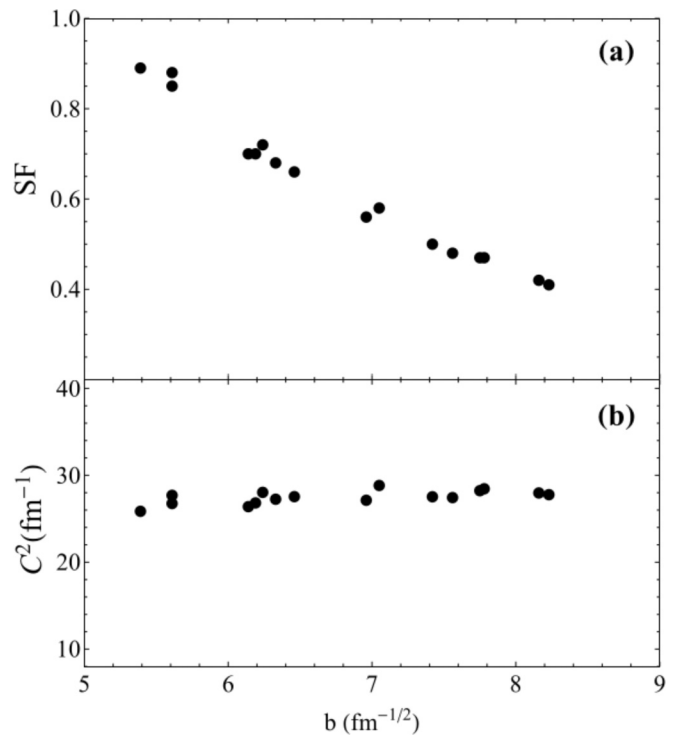


FIG. 5. (a) Spectroscopic factors and (b) ANC values extracted for the ground state of ^{27}Mg versus the value of the SPANC b . The calculations have been done using the optical potential P1.

from Guo *et al.* [18]. The discrepancies in the mirror ANC value retrieved in this work with the one from Timofeyuk *et al.* [24] is equally due to the difference between the ANC's for the $^{26}\text{Mg} + n \rightarrow ^{27}\text{Mg}^{1/2+}$ process and to the different R_{mirr} parameters used (13% in both cases). This second issue derives from the different separation energy for the proton used in the calculations, which in our case has been taken from a recent publication [26] and is equal to $S(p) = 0.807$ MeV instead of 0.859 MeV [19,24]. Using this new value, the $|C_{\text{exp}}^{1/2+}|^2$ from Timofeyuk *et al.* [24] would shift to

TABLE II. Values of the spectroscopic factors for the $^{26}\text{Mg}(d, p)^{27}\text{Mg}$ reaction and the ANC's for the $^{26}\text{Mg}(n, \gamma)^{27}\text{Mg}$ capture—for the ground and first excited states—calculated with the present experimental data (data from literature also reported). The nlj values used in the calculations are the same as reported in literature [10]. The spectroscopic factor used for the ground state is the same for P1 and P2 potentials. For the first excited state, is taken as the average of $S = 0.51$ (P1) and $S = 0.58$ (P2).

	g.s.	0.984 MeV
nlj	$1s_{1/2}$	$0d_{3/2}$
J^π	$1/2^+$	$3/2^+$
Spectroscopic factor	0.62	0.55
$C_{\text{exp}}^2 [\text{fm}^{-1}]$ [18]	44.00 ± 5.30	3.40 ± 0.32
$C_{\text{exp}}^2 [\text{fm}^{-1}]$ [24]	24.50 ± 4.90	1.10 ± 0.15
$C_{\text{exp}}^2 [\text{fm}^{-1}]$ (this work)	28.26 ± 4.24	1.41 ± 0.25

TABLE III. Comparison between the total widths Γ_p in the case when symmetry breaking is considered or not. The apexes (a) and (b) refer to the case with and without symmetry breaking, respectively. The resonance is at $E_R = 0.318$ MeV [26,27].

	This work	Ref. [24]
Γ_p [MeV]	$(5.23 \pm 1.05) \times 10^{-9}$ (a)	$(4.04 \pm 0.77) \times 10^{-9}$
	$(6.38 \pm 1.27) \times 10^{-9}$ (b)	

1230 ± 317 fm $^{-1}$, leading to a fair agreement between the central values.

The first excited state of ^{27}P is unbound, so the width Γ_p for the $^{27}\text{P}^{3/2+}$ resonance ($E_R = 0.318$ MeV) can be extracted using a relation similar to Eq. (7) [42]:

$$R_\Gamma = \frac{\Gamma_p}{|C_n|^2} \simeq R_0^{\text{res}} = \frac{\hbar^2 k_p}{\mu} \left| \frac{F_l(k_p R_N)}{k_p R_N j_l(ik_n R_N)} \right|^2. \quad (10)$$

As pointed out by Timofeyuk *et al.* [24] the nuclei $^{27}\text{Mg}^{3/2+}$ — $^{27}\text{P}^{3/2+}$ have been addressed as a candidate for mirror symmetry breaking. Using the microscopic cluster model the authors have estimated a possible realistic value of S_p/S_n , assuming that the full *sd* shell model spectroscopic factor for $^{27}\text{Mg}^{3/2+}$ is not influenced by threshold effects. They also estimated the ratio $R_\Gamma/R_0^{\text{res}}$ using the correlation between $R_\Gamma/R_0^{\text{res}}$ and C_n . This estimations suggests that the symmetry breaking in the mirror spectroscopic factors is about 18% [24]. The relation between R_Γ and R_0^{res} will therefore be $R_\Gamma = (0.82 \pm 0.05) \times R_0^{\text{res}}$. For this reason the Γ_p for the first excited state calculated in this work from the extracted C_n has been evaluated in both cases, with and without symmetry breaking, using the relation given in Ref. [24].

TABLE IV. The $^{26}\text{Si}(p, \gamma)^{27}\text{P}$ reaction rate (in $\frac{\text{cm}^3}{\text{mol} \times \text{sec}}$) for the ground-state direct capture and the first excited state resonant contribution, extracted using Eqs. (12)–(14). The present data are compared with the ones coming from [26], derived in the same way but using the different Γ_γ , Γ_p , and $S(0)$.

T_9	Reaction rate ground state (this work)				Ref. [26]	Reaction rate first excited state (this work)			
	Lower Limit	Value	Upper Limit			Lower Limit	Value	Upper Limit	Ref. [26]
0.1	8.48×10^{-14}	9.57×10^{-14}	1.25×10^{-13}		6.68×10^{-14}	2.09×10^{-12}	2.91×10^{-12}	3.84×10^{-12}	1.41×10^{-12}
0.2	2.71×10^{-09}	3.06×10^{-09}	4.01×10^{-09}		2.13×10^{-09}	7.63×10^{-05}	1.06×10^{-04}	1.40×10^{-04}	5.15×10^{-05}
0.3	4.02×10^{-07}	4.53×10^{-07}	5.94×10^{-07}		3.17×10^{-07}	1.94×10^{-02}	2.71×10^{-02}	3.58×10^{-02}	1.32×10^{-02}
0.4	9.28×10^{-06}	1.05×10^{-05}	1.37×10^{-05}		7.31×10^{-06}	2.74×10^{-01}	3.81×10^{-01}	5.03×10^{-01}	1.85×10^{-01}
0.5	8.57×10^{-05}	9.66×10^{-05}	1.27×10^{-04}		6.75×10^{-05}	1.24	1.72	2.28	8.38×10^{-01}
0.6	4.64×10^{-04}	5.24×10^{-04}	6.86×10^{-04}		3.66×10^{-04}	3.23	4.49	5.93	2.18
0.7	1.78×10^{-03}	2.01×10^{-03}	2.63×10^{-03}		1.40×10^{-04}	6.17	8.58	$1.13 \times 10^{+01}$	4.17
0.8	5.39×10^{-03}	6.08×10^{-03}	7.96×10^{-03}		4.25×10^{-03}	9.76	$1.36 \times 10^{+01}$	$1.79 \times 10^{+01}$	6.60
0.9	1.37×10^{-02}	1.54×10^{-02}	2.02×10^{-02}		1.08×10^{-02}	$1.37 \times 10^{+01}$	$1.90 \times 10^{+01}$	$2.51 \times 10^{+01}$	9.23
1.0	3.05×10^{-02}	3.44×10^{-02}	4.51×10^{-02}		2.40×10^{-02}	$1.76 \times 10^{+01}$	$2.44 \times 10^{+01}$	$3.23 \times 10^{+01}$	$1.19 \times 10^{+01}$
1.2	1.14×10^{-01}	1.28×10^{-01}	1.68×10^{-01}		8.97×10^{-02}	$2.47 \times 10^{+01}$	$3.44 \times 10^{+01}$	$4.54 \times 10^{+01}$	$1.67 \times 10^{+01}$
1.4	3.24×10^{-01}	3.66×10^{-01}	4.79×10^{-01}		2.56×10^{-01}	$3.04 \times 10^{+01}$	$4.23 \times 10^{+01}$	$5.59 \times 10^{+01}$	$2.06 \times 10^{+01}$
1.6	7.67×10^{-01}	8.65×10^{-01}	1.13		6.04×10^{-01}	$3.47 \times 10^{+01}$	$4.82 \times 10^{+01}$	$6.36 \times 10^{+01}$	$2.34 \times 10^{+01}$
1.8	1.58	1.78	2.34		1.25	$3.75 \times 10^{+01}$	$5.22 \times 10^{+01}$	$6.89 \times 10^{+01}$	$2.53 \times 10^{+01}$
2.0	2.95	3.32	4.36		2.32	$3.93 \times 10^{+01}$	$5.47 \times 10^{+01}$	$7.22 \times 10^{+01}$	$2.66 \times 10^{+01}$

The results of these calculations are reported in Table III with and without symmetry breaking, along with the one from Timofeyuk *et al.* [24].

With the above results it is possible to calculate the reaction rate for the $^{26}\text{Si} + p \rightarrow ^{27}\text{P} + \gamma$. In the following, the value of $\Gamma_p = 5.23 \times 10^{-9}$ MeV will be used for the first excited state. In general, the reaction rate can be calculated as [52]:

$$N_A \langle \sigma v \rangle = \sqrt{\frac{8}{\pi \mu}} \frac{N_A}{(kT)^{3/2}} \int_0^\infty e^{-2\pi\eta} S(E) e^{-E/kT} dE, \quad (11)$$

where μ is the reduced mass of the interacting particles, N_A the Avogadro number, k the Boltzmann constant, T the temperature, η the Sommerfeld parameter, and $S(E)$ the astrophysical *S* factor. This last quantity has been determined using the RADCAP code [53], employing a potential model for the Woods-Saxon well of the $^{26}\text{Si} + p$ compound system. The potential is adjusted to match the ANC value, the energy of the first excited state and the deduced Γ_p . This calculation shows that the $S(E)$ is roughly constant— $S(E) = S(0) = 68 \pm 12$ keV \times b—in the energy range between 0 and 1.4 MeV. This energy range was chosen considering the Gamow windows (ΔE_G) and Gamow energies (E_G) for the process at the temperatures reported in Ref. [5] ($T \approx 1 \times 10^9$ K, $E_G = 0.7$ MeV, $\Delta E_G = 0.57$ MeV), and in Ref. [7] ($T \approx 3 \times 10^8$ K, $E_G = 0.31$ MeV, $\Delta E_G = 0.2$ MeV) for the proposed astrophysical scenarios. Since the $S(E)$ is almost constant, Eq. (11) can be approximated using the relation [52]

$$N_A \langle \sigma v \rangle_{\text{DC}} = 7.8327 \times 10^9 \left(\frac{Z_{\text{Si}} Z_p}{\mu T_9^2} \right)^{1/3} S_{\text{eff}} \times \exp \left[-4.2487 \left(\frac{Z_{\text{Si}}^2 Z_p^2 \mu}{T_9} \right)^{1/3} \right] \left[\frac{\text{cm}^3}{\text{mol} \times \text{sec}} \right] \quad (12)$$

Z_{Si} and Z_p being the atomic numbers of ^{26}Si and the proton, and T_9 the temperature in units of [GK]. The quantity S_{eff} is equal to [52]

$$S_{\text{eff}} \approx S(0) \left[1 + 0.09807 \left(\frac{T_9}{Z_{\text{Si}}^2 Z_p^2 \mu} \right)^{1/3} \right]. \quad (13)$$

The proton resonance width Γ_p ($E_R = 0.318$ MeV) is small enough to be considered narrow and it is also isolated. The reaction rate will therefore be equal to [52]

$$N_A \langle \sigma v \rangle_R = \frac{1.5394 \times 10^{11}}{(\mu T_9)^{3/2}} \times \frac{2J_R + 1}{(2J_p + 1)(2J_{\text{Si}} + 1)} \frac{\Gamma_p \Gamma_\gamma}{\Gamma_p + \Gamma_\gamma} \times \exp\left(-\frac{11.605 E_R}{T_9}\right) \left[\frac{\text{cm}^3}{\text{mol} \times \text{sec}} \right], \quad (14)$$

where $J_R = 3/2$ is the spin of the resonance, E_R its energy, $J_p = 1/2$ is the spin of the proton, $J_{\text{Si}} = 0$ is the spin of the ground state of ^{26}Si , Γ_p is the proton width extracted previously (considering the case with symmetry breaking, see Table III), and Γ_γ is the γ resonance width. Regarding the latter, in Sun *et al.* [26] the authors were able to experimentally extract the ratio between the γ -ray and proton branches, $I_\gamma/I_p = \Gamma_\gamma/\Gamma_p = 1.35 \pm 0.39$. Using our value of Γ_p , the Γ_γ is therefore $\Gamma_\gamma = (7.06 \pm 1.4) \times 10^{-9}$ MeV.

The reaction rates for both the direct capture in the ground state and the first excited state resonant contributions calculated using Eqs. (12)–(14), with the $S(0)$, Γ_p and Γ_γ retrieved in this work, are reported in Table IV (with upper and lower limits). Values of both contributions to the reaction rate reported in Sun *et al.* [26] are also reported in Table IV.

A comparison between the values of the reaction rate extracted in this work and the one from Sun *et al.* [26] show an increase of the reaction rate for the $^{26}\text{Si}(p, \gamma)^{27}\text{P}$ of a factor 1.4 for the ground state and 2.2 for the first excited state, respectively.

V. CONCLUSIONS

We determined the values of the ANC's for the $^{26}\text{Mg} + n \rightarrow ^{27}\text{Mg}$ neutron capture reaction populating the ground

and the first excited states of ^{27}Mg from the $^{26}\text{Mg}(d, p)^{27}\text{Mg}$ reaction. Also, the ANC for the direct capture in the ground state and the width Γ_p for the first excited state of ^{27}P populated by means of the $^{26}\text{Si}(p, \gamma)^{27}\text{P}$ reaction have been extracted, using the well-established procedure for mirror nuclei [19–23]. The symmetry breaking effect for the first excited state suggested by Timofeyuk *et al.* [24] is included in the present calculation. The observed effect is within our experimental errors (see Table III). More experimental data regarding the $^{26}\text{Si} + p \rightarrow ^{27}\text{P}$ reaction—either using direct or indirect methods—directly involving ^{26}Si in the entrance channel would shed a light on the problem. Such experiments nonetheless are challenging, because of the short half-life of ^{26}Si (2.24 sec). The presented measurement of the ANC values of the $^{26}\text{Mg}(n, \gamma)^{27}\text{Mg}$ reaction turned out to be higher than those reported in Timofeyuk *et al.* [24]. This could be due to the well-known sensitivity of (d, p) reactions to high n - p momenta [54]. Therefore, improved calculations performed using adiabatic distorted wave approximation and continuum-discretized coupled-channel approaches on our experimental data would be very useful. The reaction rate for the direct capture to the ground state and the first excited state resonant contribution have been also deduced. The former has been calculated using our experimentally extracted ANC for the $^{26}\text{Si} + p \rightarrow ^{27}\text{P}$. The latter was calculated using our independently measured Γ_p and the new experimentally measured ratio Γ_γ/Γ_p [26,27]. Higher values in both quantities have been obtained (see Table IV). An evaluation of the impact of this augmented reaction rate in the stellar scenarios is of interest.

ACKNOWLEDGMENTS

This work was supported by MEYS Czech Republic under the project SPIRAL2-CZ, EF16_013/0001679. The authors also want to thank the efforts of the target laboratory of the INFN - LNS in producing the ^{26}Mg targets, and Prof. Carlos Bertulani for the RADCAP code and fruitful discussions.

-
- [1] W. A. Mahoney, J. C. Ling, A. S. Jacobson, and R. E. Lingenfelter, *Astrophys. J.* **262**, 745 (1982).
 - [2] R. Diehl, C. Dupraz, K. Bennett, H. Bloemen, W. Hermsen, J. Knoedlseder, G. Lichti, D. Morris, J. Ryan, V. Schoenfelder, H. Steinle, A. Strong, B. Swanenburg, M. Varendorff, and C. Winkler, *A & A* **298**, 445 (1995).
 - [3] W. Chen, N. Gehrels, and R. Diehl, *Astrophys. J. Lett.* **440**, L57 (1995).
 - [4] L. Bouchet, E. Jourdain, and J.-P. Roques, *Astrophys. J.* **801**, 142 (2015).
 - [5] N. Prantzos and R. Diehl, *Phys. Rep.* **267**, 1 (1996).
 - [6] J. José, A. Coc, and M. Hernanz, *Astrophys. J.* **560**, 897 (2001).
 - [7] O. Koike, M. Hashimoto, K. Arai, and S. Wanajo, *A & A* **342**, 464 (1999).
 - [8] C. Angulo, M. Arnould, M. Rayet, P. Descouvemont, D. Baye, C. Leclercq-Willain, A. Coc, S. Barhoumi, P. Aguer, C. Rolfs, R. Kunz, J. W. Hammer, A. Mayer, T. Paradellis, S. Kossionides *et al.*, *Nucl. Phys. A* **656**, 3 (1999).
 - [9] A. Coc, M. G. Porquet, and F. Nowacki, *Phys. Rev. C* **61**, 015801 (1999).
 - [10] M. S. Basunia and A. M. Hurst, *Nucl. Data Sheets* **134**, 1 (2016).
 - [11] M. Wiescher, J. Görres, F.-K. Thielemann, and H. Ritter, *A & A* **160**, 56 (1986).
 - [12] H. Herndl, J. Görres, M. Wiescher, B. A. Brown, and L. Van Wormer, *Phys. Rev. C* **52**, 1078 (1995).
 - [13] J. A. Caggiano, D. Bazin, W. Benenson, B. Davids, R. Ibbotson, H. Scheit, B. M. Sherrill, M. Steiner, J. Yurkon, A. F. Zeller, B. Blank, M. Chartier, J. Greene, J. A. Nolen, A. H. Wuosmaa *et al.*, *Phys. Rev. C* **64**, 025802 (2001).
 - [14] Y. Togano, T. Gomi, T. Motobayashi, Y. Ando, N. Aoi, H. Baba, K. Demichi, Z. Elekes, N. Fukuda, Z. Fulop, U. Futakami,

- H. Hasegawa, Y. Higurashi, K. Ieki, N. Imai, M. Ishihara, K. Ishikawa, N. Iwasa, H. Iwasaki, S. Kanno, Y. Kondo, T. Kubo, S. Kubono, M. Kunibu, K. Kurita, Y. U. Matsuyama, S. Michimasa, T. Minemura, M. Miura, H. Murakami, T. Nakamura, M. Notani, S. Ota, A. Saito, H. Sakurai, M. Serata, S. Shimoura, T. Sugimoto, E. Takeshita, S. Takeuchi, K. Ue, K. Yamada, Y. Yanagisawa, K. Yoneda, and A. Yoshida, *Phys. Rev. C* **84**, 035808 (2011).
- [15] Y. Togano, T. Gomi, T. Motobayashi, Y. Ando, N. Aoi, H. Baba, K. Demichi, Z. Elekes, N. Fukuda, Z. Fülöp, U. Futakami, H. Hasegawa, Y. Higurashi, K. Ieki *et al.*, in *Origin of Matter and Evolution of Galaxies 2003* (World Scientific, Singapore, 2005).
- [16] J. Marganec, S. Beceiro Novo, S. Typel, C. Langer, C. Wimmer, H. Alvarez-Pol, T. Aumann, K. Boretzky, E. Casarejos, A. Chatillon, D. Cortina-Gil, U. Datta-Pramanik, Z. Elekes, Z. Fülöp, D. Galaviz, H. Geissel, S. Giron, U. Greife, F. Hammache, M. Heil, J. Hoffman, H. Johansson, O. Kiselev, N. Kurz, K. Larsson, T. Le Bleis, Y. A. Litvinov, K. Mahata, C. Muentz, C. Nociforo, W. Ott, S. Paschalis, R. Plag, W. Prokopowicz, C. Rodríguez Tajés, D. M. Rossi, H. Simon, M. Stanoiu, J. Stroth, K. Sümmerer, A. Wagner, F. Wamers, H. Weick, and M. Wiescher (R3B Collaboration), *Phys. Rev. C* **93**, 045811 (2016).
- [17] F. Meurders and A. Van Der Steld, *Nucl. Phys. A* **230**, 317 (1974).
- [18] Guo, B., Z. H. Li, X. X. Bai, W. P. Liu, N. C. Shu, and Y. S. Chen, *Phys. Rev. C* **73**, 048801 (2006).
- [19] N. K. Timofeyuk, R. C. Johnson, and A. M. Mukhamedzhanov, *Phys. Rev. Lett.* **91**, 232501 (2003).
- [20] L. Trache, A. Azhari, F. Carstou, H. L. Clark, C. A. Gagliardi, Y. W. Liu, A. M. Mukhamedzhanov, X. Tang, N. Timofeyuk, and R. E. Tribble, *Phys. Rev. C* **67**, 062801(R) (2003).
- [21] T. Al-Abdullah, F. Carstou, X. Chen, H. L. Clark, C. A. Gagliardi, Y.-W. Lui, A. Mukhamedzhanov, G. Tabacaru, Y. Tokimoto, L. Trache, R. E. Tribble, and Y. Zhai, *Phys. Rev. C* **89**, 025809 (2014).
- [22] M. McCleskey, A. M. Mukhamedzhanov, L. Trache, R. E. Tribble, A. Banu, V. Eremenko, V. Z. Goldberg, Y.-W. Lui, E. McCleskey, B. T. Roeder, A. Spiridon, F. Carstou, V. Burjan, Z. Hons, and I. J. Thompson, *Phys. Rev. C* **89**, 044605 (2014).
- [23] A. M. Mukhamedzhanov, *Phys. Rev. C* **99**, 024311 (2019).
- [24] N. K. Timofeyuk, P. Descouvemont, and I. J. Thompson, *Phys. Rev. C* **78**, 044323 (2008).
- [25] R. C. Johnson and P. J. Soper, *Phys. Rev. C* **1**, 976 (1970).
- [26] L. J. Sun, X. X. Xu, C. J. Lin, J. Lee, S. Q. Hou, C. X. Yuan, Z. H. Li, J. José, J. J. He, J. S. Wang, D. X. Wang, H. Y. Wu, P. F. Liang, Y. Y. Yang, Y. H. Lam, P. Ma, F. F. Duan, Z. H. Gao, Q. Hu, Z. Bai, J. B. Ma, J. G. Wang, F. P. Zhong, C. G. Wu, D. W. Luo, Y. Jiang, Y. Liu, D. S. Hou, R. Li, N. R. Ma, W. H. Ma, G. Z. Shi, G. M. Yu, D. Patel, S. Y. Jin, Y. F. Wang, Y. C. Yu, Q. W. Zhou, P. Wang, L. Y. Hu, X. Wang, H. L. Zang, P. J. Li, Q. Q. Zhao, L. Yang, P. W. Wen, F. Yang, H. M. Jia, G. L. Zhang, M. Pan, X. Y. Wang, H. H. Sun, Z. G. Hu, R. F. Chen, M. L. Liu, W. Q. Yang, Y. M. Zhao, and H. Q. Zhang (RIBLL Collaboration), *Phys. Rev. C* **99**, 064312 (2019).
- [27] L. J. Sun, X. X. Xu., S. Q. Hou, C. J. Lin, J. José, J. Lee, J. J. He, Z. H. Li, J. S. Wang, C. X. Yuan, F. Herwig, J. Keegans, T. Budner, D. X. Wang, H. Y. Wu, P. F. Liang, Y. Y. Yang, Y. H. Lam, P. Ma, F. F. Duan, Z. H. Gao, Q. Hu, Z. Bai, J. B. Ma, J. G. Wang, F. P. Zhong, C. G. Wu, D. W. Luo, Y. Jiang, Y. Liu, D. S. Hou, R. Li, N. R. Ma, W. H. Ma, G. Z. Shi, G. M. Yu, D. Patel, S. Y. Jin, Y. F. Wang, L. Y. Hu, X. Wang, H. L. Zang, P. J. Li, Q. Q. Zhao, H. M. Jia, L. Yang, P. W. Wen, F. Yang, M. Pan, X. Y. Wang, Z. G. Hu, R. F. Chen, M. L. Liu, W. Q. Yang, and Y. M. Zhao, *Phys. Lett. B* **802**, 135213 (2020).
- [28] C. Iliadis, R. Longland, A. E. Champagne, and A. Coc, *Nucl. Phys. A* **841**, 251 (2010).
- [29] I. J. Thompson, *Comput. Phys. Rep.* **7**, 167 (1988).
- [30] R. E. Tribble, C. A. Bertulani, M. La Cognata, A. M. Mukhamedzhanov, and C. Spitaleri, *Rep. Prog. Phys.* **77**, 106901 (2014).
- [31] G. Baur, C. A. Bertulani, and H. Rebel, *Nucl. Phys. A* **458**, 188 (1986).
- [32] C. Spitaleri, in *Problems of Fundamental Modern Physics II: Proceedings*, edited by R. Cherubini, P. Dalpiaz, and B. Minetti (World Scientific, Singapore, 1991), p. 21.
- [33] C. Spitaleri, M. La Cognata, L. Lamia, A. M. Mukhamedzhanov, and R. G. Pizzone, *Eur. Phys. J. A* **52**, 77 (2016).
- [34] L. D. Blokhintsev, I. Borbely, and E. I. Dolinskii, *Sov. J. Part. Nucl.* **8**, 485 (1977).
- [35] A. M. Mukhamedzhanov and N. K. Timofeyuk, *JETP. Lett* **51**, 282 (1990).
- [36] H. M. Xu, C. A. Gagliardi, R. E. Tribble, A. M. Mukhamedzhanov, and N. K. Timofeyuk, *Phys. Rev. Lett.* **73**, 2027 (1994).
- [37] V. Burjan, Z. Hons, V. Kroha, J. Mrázek, Š. Piskoř, A. M. Mukhamedzhanov, L. Trache, R. E. Tribble, M. La Cognata, L. Lamia, R. G. Pizzone, S. Romano, C. Spitaleri, and A. Tumino, *Eur. Phys. J. A* **55**, 114 (2019).
- [38] A. M. Mukhamedzhanov, V. Burjan, M. Gulino, Z. Hons, V. Kroha, M. McCleskey, J. Mrázek, N. Nguyen, F. M. Nunes, v. Piskoř, S. Romano, M. L. Sergi, C. Spitaleri, and R. E. Tribble, *Phys. Rev. C* **84**, 024616 (2011).
- [39] G. G. Kiss, M. La Cognata, C. Spitaleri, R. Yarmukhamedov, I. Wiedenhöver, L. T. Baby, S. Cherubini, A. Cvetinović, G. D'Agata, P. Figuera, G. L. Guardo, M. Gulino, S. Hayakawa, I. Indelicato, L. Lamia, M. Lattuada, F. Mudò, S. Palmerini, R. G. Pizzone, G. G. Rapisarda, S. Romano, M. L. Sergi, R. Sparta, O. Trippella, A. Tumino, M. Anastasiou, S. A. Kuvin, N. Rijal, B. Schmidt, S. B. Igamov, S. B. Sakuta, K. I. Tursunmakhatov, Z. Fülöp, G. Gyürky, T. Szücs, Z. Halász, E. Somorjai, Z. Hons, J. Mrázek, R. E. Tribble, and A. M. Mukhamedzhanov, *Phys. Lett. B* **807**, 135606 (2020).
- [40] G. R. Satchler, *Direct Nuclear Reactions*, International Series of Monographs on Physics (Clarendon Press, Oxford, 1983).
- [41] A. M. Mukhamedzhanov, H. L. Clark, C. A. Gagliardi, Y. W. Lui, L. Trache, R. E. Tribble, H. M. Xu, X. G. Zhou, V. Burjan, J. Cejpek, V. Kroha, and F. Carstou, *Phys. Rev. C* **56**, 1302 (1997).
- [42] N. K. Timofeyuk and S. B. Igamov, *Nucl. Phys. A* **713**, 217 (2003).
- [43] P. D. Kunz, Instruction for the use of DWUCK: A Distorted Wave Born Approximation Program, Technical Report NSA-24-026673 (United States, 1969), <https://www.osti.gov/biblio/4157791>.
- [44] S. A. Goncharov, J. Dobesh, E. I. Dolinskii, A. M. Mukhamedzhanov, and J. Cejpek, *Sov. J. Nucl. Phys.* **35**, 383 (1982).

- [45] Z. H. Liu, C. J. Lin, H. Q. Zhang, Z. C. Li, J. S. Zhang, Y. W. Wu, F. Yang, M. Ruan, J. C. Liu, S. Y. Li, and Z. H. Peng, *Phys. Rev. C* **64**, 034312 (2001).
- [46] A. M. Mukhamedzhanov and F. M. Nunes, *Phys. Rev. C* **72**, 017602 (2005).
- [47] T. L. Belyaeva, R. Perez-Torres, A. A. Ogloblin, A. S. Demyanova, S. N. Ershov, and S. A. Goncharov, *Phys. Rev. C* **90**, 064610 (2014).
- [48] J. Yang and P. Capel, *Phys. Rev. C* **98**, 054602 (2018).
- [49] R. V. Reid, *Ann. Phys.* **50**, 411 (1968).
- [50] A. M. Mukhamedzhanov, F. M. Nunes, and P. Mohr, *Phys. Rev. C* **77**, 051601(R) (2008).
- [51] N. B. Nguyen, F. M. Nunes, and R. C. Johnson, *Phys. Rev. C* **82**, 014611 (2010).
- [52] C. Iliadis, *Nuclear Physics of Stars* (Wiley-VCH Verlag, New York, 2007).
- [53] C. A. Bertulani, *Comput. Phys. Commun.* **156**, 123 (2003).
- [54] G. W. Bailey, N. K. Timofeyuk, and J. A. Tostevin, *Phys. Rev. C* **95**, 024603 (2017).